Diffusion Effects in the Inhomogeneously Broadened Case: High-Temperature Saturation of the *F*-Center Electron Spin Resonance*

E. L. Wolf†
Department of Physics, Cornell University, Ithaca, New York
(Received 17 September 1965)

An experimental and theoretical study is made of the effects of a random spectral diffusion process on the saturation behavior of a normally inhomogeneously broadened resonance. The random type of spectral diffusion process results, for example, if a spin diffuses on a set of sites having a distribution of local fields giving the inhomogeneous width but such that local fields at adjacent sites are uncorrelated. The calculation shows a transition in saturation properties to those characteristic of a homogeneously broadened resonance as the quantity $\beta=\omega_D(\omega_1+\omega_D)/\omega_1\omega_2^*$ approaches unity, where ω_1, ω_D, and ω_2^* represent, respectively, the spin-lattice relaxation rate, the spectral diffusion rate, and the inhomogeneous width. A study of the transition behavior can yield values of ω_1 and ω_D in the transition range. The analysis is shown to apply in the transition range 470 to 550°C for the KCl *F* center. Analysis of the transition saturation data yields a value of ω_1 which agrees with the expression of Feldman, Warren, and Castle, which for absolute temperatures T large compared with 210°K becomes $\omega_1=3.5\times10^{-1}T^2$ sec^{-1}. The spectral diffusion rate in zone-refined samples is given by $\omega_D=12\,\nu_0\exp(-E_m/kT)$, where $\nu_0=3.7\times10^{15}\times10^{\pm1.2}$ sec^{-1}, and $E_m=1.6\pm0.2$ eV. The spectral diffusion is interpreted as resulting from diffusion of the *F* center in [110] steps of length $\sqrt{2}a$, where a is the interionic distance, with attempt frequency ν_0 and motion energy E_m. This process does not account for the diffusion coefficient of the *F* center, which results from diffusion of ionized electrons to anion vacancies, and which is limited in the case of dense coloration by charge compensating vacancy diffusion.

I. INTRODUCTION

INVESTIGATIONS of the magnetic resonance of the *F* center[1–6] have given conclusive support to the model of an electron bound by an anion vacancy and have more recently provided a detailed knowledge of the interaction of the electron spin with the nuclear moments of its neighbor ions, and through the latter, its interaction with the lattice vibrations.[7] These recent investigations have verified that the unusually large width of the nearly Gaussian absorption spectrum arises from unresolved hyperfine interaction with the first few shells of neighboring nuclei. The main features of the saturation behavior of the resonance, or dependence of the absorption signal $H_1\chi''$ on the square H_1^2 of the exciting resonant magnetic field, were explained by Portis[8] on the assumption that hyperfine interaction with near neighbors is static. In this case, the near neighbor hyperfine interaction can be regarded as producing a static local field $H_{\rm loc}$ which determines the transition frequency of the electron at a particular site. Electrons having a particular local field and hence a particular resonant frequency, $\omega=\gamma(H_0+H_{\rm loc})$ within the inhomogeneous distribution, where γ is the gyromagnetic ratio, belong to the same spin packet. The width $\omega_2=1/T_2$ of a packet (small compared with ω_2^*, a measure of the width of the $\gamma H_{\rm loc}$ distribution) is determined by time-dependent interactions of the spins. In the simplest case, ω_2 arises from uncertainty or lifetime broadening (e.g., by spin-lattice interaction); the spin-packet at frequency ω' is described by the Lorentzian

$$g(\omega-\omega')=\frac{1}{\pi}\frac{\omega_2}{\omega_2^2+(\omega-\omega')^2}. \tag{1.1}$$

Portis[8] showed for the case of an inhomogeneous distribution of Lorentzian spin packets that $H_1\chi''$ saturates at $(\gamma H_{1/2})^2=\omega_1\omega_2$, where $\omega_1=1/T_1$ is the spin-lattice relaxation rate, and that for $H_1>H_{1/2}$ $H_1\chi''$ tends toward at constant value, in contrast to the homogeneously broadened case in which $H_1\chi''\propto1/H_1$ for $H_1>H_{1/2}$. The increased signal $H_1\chi''$ in the inhomogeneously broadened case for $H_1>H_{1/2}$ is the result of absorption by spin packets somewhat displaced from the driving frequency ω_0. By Eq. (1.1) these interact less strongly with the excitation and thus a larger value of H_1 is required to lower significantly the population difference of the states split by $\hbar\omega$.

Subsequent extension of saturation measurements at room temperature to much higher values of power H_1^2 revealed[9–11] a decrease of $H_1\chi''$ (beyond saturation) from the constant value predicted by the Portis theory. This "droop" results, in part, from failure of the assumption of Lorentzian spin packets, which is believed to result from time-dependent hyperfine interaction with more distant Cl^- neighbors located in [211]

* Work supported by the U. S. Atomic Energy Commission under Contract AT(30-1)-2150.
† Present address: Department of Physics, University of Illinois, Urbana, Illinois.
[1] A. F. Kip, C. Kittel, R. A. Levy, and A. M. Portis, Phys. Rev. **91**, 1066 (1953).
[2] G. Feher, Phys. Rev. **105**, 1122 (1957).
[3] W. C. Holton and H. Blum, Phys. Rev. **125**, 89 (1962).
[4] W. T. Doyle, Phys. Rev. **126**, 1421 (1962).
[5] H. Seidel, Z. Physik, **165**, 218, 239 (1961).
[6] P. R. Moran, Phys. Rev. **135**, A247 (1964).
[7] D. W. Feldman, R. W. Warren, and J. G. Castle, Jr., Phys. Rev. **135**, A470 (1964).
[8] A. M. Portis, Phys. Rev. **91**, 1071 (1953).
[9] P. R. Moran, S. H. Christensen, and R. H. Silsbee, Phys. Rev. **124**, 442 (1961).
[10] H. C. Wolf and H. Gross, Naturwiss. **8**, 299 (1961).
[11] P. R. Moran, Ph.D. thesis, Cornell University, 1963 (unpublished).

directions.[6] As the 24 [211] shell Cl^- nuclei interacting with the lattice vibrations undergo $\Delta M_I = \pm 1$ transitions at a rate ω_N, the hyperfine coupling causes discrete diffusion of the electron resonant frequency which may be regarded as a random walk in frequency at step rate $24\omega_N$ and with short step length $\Delta\omega_j$. The estimate of ω_2 suggested by Moran[6] for this picture is $\omega_2{}^e \approx (DT_1)^{1/2}$, where the diffusion constant D is $24\omega_N(\Delta\omega_j)^2$ and the random walk persists for an electronic spin-lattice relaxation time.

In this paper we describe an investigation of the magnetic resonance of the F center in the temperature range from room temperature to 550°C. This work has had two motivations. The first has been to check the detailed model of the resonance resulting from the work of Feldman *et al.*,[7] and Moran,[6] by measuring the temperature dependence of the relaxation parameters over an extended range. Specifically, Feldman *et al.* predict that the spin-lattice relaxation rate should increase as the square of the absolute temperature for temperatures above 210°K. Moran has suggested that the effective packet width

$$\omega_2{}^e = (24\omega_N/\omega_1)^{1/2}\Delta\omega_j$$

may be independent of temperature in ranges where the temperature dependence of the electronic spin-lattice relaxation rate and the spin-lattice relaxation rate of the [211] Cl^- nuclei are identical.

The second and major objective has been to study possible effects of defect diffusion on the resonance behavior. It has long been known that at 500°C and higher the F center has an anomalously high diffusion coefficient,[12] as measured by motion of the visible coloration, and that the F center coloration drifts in an applied electric field. Since an F center is electrically neutral, the latter observation suggests a process of thermal ionization of the electron, which then drifts in the conduction band and is recaptured at a distant anion vacancy. A second diffusion process occurs when an F center and one of its twelve nearest [110] Cl^- neighbors exchange positions. To avoid confusion, we call the latter process F center step diffusion. A further possibility is that diffusion of other defects, such as lattice vacancies, near the F center may affect the resonance. The cation vacancy has a jump rate of the order of 10^{10} sec^{-1} at 550°C and could affect the resonance by rearranging the potassium ions near an F center.

Important diffusion effects are in fact observed. An interesting feature in the high-temperature resonance data is a systematic trend from saturation behavior appropriate to an inhomogeneously broadened resonance to that expected in cases of homogeneous broadening. Although such a transition could result from an increasing level width violating the condition $\omega_2 \ll \omega_2{}^*$,[13] in the present case it is believed to be a consequence of spectral diffusion caused by defect motion.

[12] R. W. Pohl, Proc. Phys. Soc. (London) **49**, 3 (1937).
[13] T. G. Castner, Jr., Phys. Rev. **115**, 1506 (1959).

In fact, the two modes of F center diffusion described above produce an especially simple diffusion of the transition frequency of the electron spin.[14] After such an event, the electron sees a new set of neighbor nuclei; to a first approximation the final resonant frequency of the electron is uncorrelated with its initial value and is distributed at random within the Gaussian resonance absorption lineshape. The rms frequency change is large, of the order of the inhomogeneous width $\omega_2{}^*$; hence the diffusion contributes a lifetime broadening to the spin packet, which may be dominant at sufficiently high temperature. In this instance the spin-packet function approaches the simple Lorentzian form with $\omega_2 = \omega_1 + \omega_D$.

We find that main effects on the resonance behavior as ω_D increases from ω_1 to $\omega_2{}^*$ are, in the order of their appearance: an enhanced saturation power $(\gamma H_{1/2})^2$; a transition in saturation behavior to that of a homogeneously broadened resonance when ω_D is so fast as to equalize the degree of saturation across the line; and the eventual narrowing of the line at $\omega_D \gtrsim \omega_2{}^*$. All of these effects are treated explicitly or are strongly implied in the literature of spectral diffusion[15–18] and cross relaxation.[19] What is unusual (and apparently unrecognized) about the random type of spectral diffusion is that expressions for the resulting saturation curves can be derived easily, allowing one to analyze data for the spectral diffusion and spin-lattice relaxation rates. In Sec. II, for example, we discuss an expression for $H_1\chi''$ at the center of a Gaussian inhomogeneous line which quantitatively reflects all of the effects mentioned above.

Section III describes experimental methods used to obtain saturation data up to 550°C, which is presented in IV, and interpreted in terms of the spectral diffusion model. A discussion of mechanisms and conclusions follows in V and VI. We turn now to a treatment of the spectral diffusion model.

II. EFFECTS OF SPECTRAL DIFFUSION ON INHOMOGENEOUS SATURATION

In this section, a detailed treatment of saturation on a simple model of spectral diffusion, suggested by the case of F center diffusion, is developed. The qualitative effects of some variations on this model are then briefly discussed, in order to assess the usefulness of saturation measurements in identifying spectral diffusion.

[14] The diffusion event does *not* necessarily contribute significantly to the electronic spin-lattice relaxation rate ω_1.
[15] A. M. Portis, Phys. Rev. **104**, 584 (1956).
[16] P. W. Anderson, J. Phys. Soc. Japan **9**, 316 (1954).
[17] W. B. Mims, K. Nassau, and J. D. McGee, Phys. Rev. **123**, 2059 (1961).
[18] J. R. Klauder and P. W. Anderson, Phys. Rev. **125**, 912 (1962).
[19] N. Bloembergen, S. Shapiro, P. S. Pershan, and J. O. Artman, Phys. Rev. **114**, 445 (1959).

A. Saturation on a Model of Random Spectral Diffusion

Application of a static magnetic field H_0 to a sample containing N electron spins splits the electron $M_s=\pm\frac{1}{2}$ levels by

$$\hbar\omega=\hbar[\omega_0+\gamma H_{\rm loc}], \tag{2.1}$$

where $\omega_0=\gamma H_0$ and where $H_{\rm loc}$ represents the static interaction leading to inhomogeneous broadening. The distribution in values of $\gamma H_{\rm loc}$ is given by a normalized envelope function $h(\omega)$ which essentially determines the shape of the resonance centered at ω_0. The relative populations of the $M_s=\pm\frac{1}{2}$ levels, split by $\hbar\omega$, are taken as $\frac{1}{2}[1+n(\omega)]$ and $\frac{1}{2}[1-n(\omega)]$, where $n(\omega)$ has the thermal equilibrium value

$$n(\omega)=n_0=\tanh\frac{\hbar\omega}{2kT}\cong\frac{\hbar\omega_0}{2kT}. \tag{2.2}$$

Thus the population difference for electrons having $\Delta M_s=\pm1$ transition frequencies in the range $\Delta\omega$ at ω is $Nh(\omega)n(\omega)\Delta\omega$. Application of an oscillating rf magnetic field (perpendicular to H_0),

$$H_1(t)=2H_1\sin\omega_{\rm rf}t, \tag{2.3}$$

of which only the circularly polarized component rotating in the Larmor sense is important, induces $\Delta M_s=\pm1$ transitions of spins having resonant frequencies near $\omega_{\rm rf}$ and is opposed by relaxation processes which attempt to restore the thermal equilibrium value $n(\omega)=n_0$.

The action of the spin-lattice interaction is described by the relaxation rate $\omega_1=1/T_1$, such that

$$dn(\omega)/dt|_{\rm S.L.}=-[n(\omega)-n_0]\omega_1. \tag{2.4}$$

The specific action of spectral diffusion on the random model is to cause the resonant frequency of an electron to change suddenly, after a lifetime $1/\omega_D$, from its initial value to a new value distributed simply by the envelope function $h(\omega)$. It is assumed that there are no other time-dependent interactions coupling to the spins, in particular that the electron spins are independent of each other. In this case the spin-packet width is determined by ω_1 and ω_D. The important fact that the rms frequency change $\Delta\omega_j$ in a diffusion event is large, of the order of the width ω_2* of the inhomogeneous envelope function $h(\omega)$, makes plausible the result correct for $\omega_D\ll\omega_2$*: that ω_D simply contributes to a lifetime spin transition broadening $\omega_1+\omega_D$. The spin packet at ω' is described in this case by a normalized Lorentzian function[20]

$$g(\omega-\omega')=\frac{1}{\pi}\frac{\omega_1+\omega_D}{(\omega_1+\omega_D)^2+(\omega-\omega')^2}. \tag{2.5}$$

We proceed to calculate the steady-state population difference $n_s(\omega)$ by solving a rate equation, using first-order perturbation theory for the transition rate induced by $H_1(t)$. Having obtained $n_s(\omega)$, the power absorbed is

$$P_a=-\tfrac{1}{2}N\hbar\omega_0\int_{-\infty}^{\infty}h(\omega')[n_s(\omega')-n_0]\omega_1 d\omega', \tag{2.6}$$

i.e., the rate at which the spin-lattice interaction transfers energy to the lattice. The rate equation for the population difference is

$$\begin{aligned}\frac{d}{dt}[Nh(\omega)n(\omega)]=&\frac{N(\gamma H_1)^2(\omega_1+\omega_D)h(\omega)n(\omega)}{(\omega_1+\omega_D)^2+(\omega-\omega_{\rm rf})^2}\\&-Nh(\omega)[n(\omega)-n_0]\omega_1\\&-Nh(\omega)n(\omega)\omega_D+Nh(\omega)\omega_D\\&\times\int_{-\infty}^{\infty}h(\omega')n(\omega')d\omega'=0,\end{aligned} \tag{2.7}$$

where the first two terms represent transitions induced by the rf and by the spin-lattice interaction, respectively. The last two terms represent rates of change of population difference at ω by scattering of spins away from ω, and by return scattering from all other frequencies. The last term is the total rate of change of population difference due to scattering at all points in the line multiplied by $h(\omega)$, the fraction of the scattered spins which come to the frequency ω.

That this inhomogeneous integral equation can be solved trivally[21] is a result of the uncorrelated nature of the spectral diffusion. In order to obtain $n(\omega)$, we notice that the integral is independent of ω. The complete ω dependence of $n_s(\omega)$ comes from regarding the integral as a constant to be evaluated, and simply solving for $n(\omega)$. One finds easily

$$\begin{aligned}n_s(\omega)=&n_0\frac{1}{1+S}\\&\times\left[1-\frac{(\gamma H_1)^2}{(\omega_1+\omega_D)^2+(\gamma H_1)^2+(\omega-\omega_{\rm rf})^2}\right],\end{aligned} \tag{2.8}$$

where

$$\begin{aligned}S=&\frac{\omega_D}{\omega_1}(\gamma H_1)^2\\&\times\int_{-\infty}^{\infty}\frac{h(\omega')d\omega'}{(\omega_1+\omega_D)^2+(\gamma H_1)^2+(\omega'-\omega_{\rm rf})^2}.\end{aligned} \tag{2.9}$$

The driving field thus produces a sharp reduction in n_s

[20] The failure of this approximation for $\omega_D\simeq\omega_2$* arises from phase coherence of the spins which leads to the phenomenon of motional narrowing. (It is assumed that the diffusion event is so sudden that the phase of a spin is unchanged.) A treatment based on the spin-$\frac{1}{2}$ density matrix can be carried out for saturation even in the limit $\omega_D>\omega_2$*; this treatment justifies the choice of a Lorentzian $g(\omega)$ for the case $\omega_D\ll\omega_2$*.

[21] F. B. Hildebrand, *Methods of Applied Mathematics* (Prentice Hall, Inc., Englewood Cliffs, New Jersey, 1958), p. 381.

near the frequency $\omega=\omega_{rf}$. The important effect of random spectral diffusion, reflected by the factor $1/(1+S)$ in Eq. (2.8), is to reduce the population difference *at all frequencies* by an amount depending on ω_D and $(\gamma H_1)^2$. Although S is independent of ω, it does depend, through the integral, on the difference between the driving frequency ω_{rf} and the line center ω_0.

Using (2.6), the absorbed power is

$$P_a(\omega_{rf})=\tfrac{1}{2}\hbar\omega_0 n_0\omega_1(1+\omega_1/\omega_D)(S/(1+S))N. \quad (2.10)$$

The absorption signal $H_1\chi''$, where χ'' is the loss part of the rf susceptibility, can be obtained from the relation $P_a=2\omega_0\chi''H_1^2$. The integral in (2.9) can be evaluated for a Gaussian $h(\omega)$ only at the line center, $\omega_{rf}=\omega_0$.[13] In the limit of strong inhomogeneous broadening $\omega_D\ll\omega_2^*$, however, $h(\omega)$ varies slowly in the region at ω_{rf} of width $[(\omega_1+\omega_D)^2+(\gamma H_1)^2]^{1/2}$ over which the Lorentzian function in the integral of (2.9) is large. In this limit, a good approximation in the experiments to be described, we can take $h(\omega)$ outside the integral sign as $h(\omega_{rf})$. The remaining integral is evaluated, and we find

$$S\cong(\omega_D/\omega_1)(\gamma H_1)^2h(\omega_{rf})\pi[(\omega_1+\omega_D)^2+(\gamma H_1)^2]^{-1/2}$$
$$=\left[\frac{\omega_D(\omega_1+\omega_D)}{\omega_1\omega_2^*}\frac{h(\omega_{rf})}{h(\omega_0)}\right]\frac{x^2}{(1+x^2)^{1/2}}, \quad (2.11)$$

where $\omega_2^*=(1/\pi)h(\omega_0)$ and $x=\gamma H_1/(\omega_1+\omega_D)$. The bracket term, which we denote by β, has a simple physical interpretation: it is the probability that a spin initially resonant at $\omega=\omega_{rf}$ and having diffused away will diffuse back to within $\omega_1+\omega_D$ of ω_{rf} in a spin-lattice lifetime. The average number of random scattering events in this time is ω_D/ω_1, and the rest of the bracket is the probability per jump of coming back into ω_{rf}. In this approximation the expression for $H_1\chi''(\omega)$, from (2.10), is

$$H_1\chi''(\omega)=\frac{1}{2\pi}\frac{\chi_0\omega_0}{\gamma}(\omega_1+\omega_D)\frac{xh(\omega)}{(1+x^2)^{1/2}+\beta x^2}, \quad (2.12)$$

where

$$\beta=\frac{\omega_D(\omega_1+\omega_D)}{\omega_1\omega_2^*}\frac{h(\omega)}{h(\omega_0)}. \quad (2.13)$$

Here χ_0 is the static Curie susceptibility for N electron spins, and the subscript rf has been dropped. We first remark on the lineshape of $H_1\chi''(\omega)$ before discussing the saturation behavior, or dependence on $x=\gamma H_1/(\omega_1+\omega_D)$. For the case $\beta=0$, $H_1\chi''(\omega)$ is proportional to the inhomogeneous broadening function $h(\omega)$. In the case $\beta x^2\geq(1+x^2)^{1/2}$, however, the ω dependence in β results in a flattening of the absorption near $\omega=\omega_0$. We have not been primarily interested in this effect, which is not as noticeable for smaller β as changes in the saturation. We note, however, that the usual assumption of proportionality between the absorption $H_1\chi''(\omega_0)$ and the peak derivative signal is not strictly correct, in this situation.

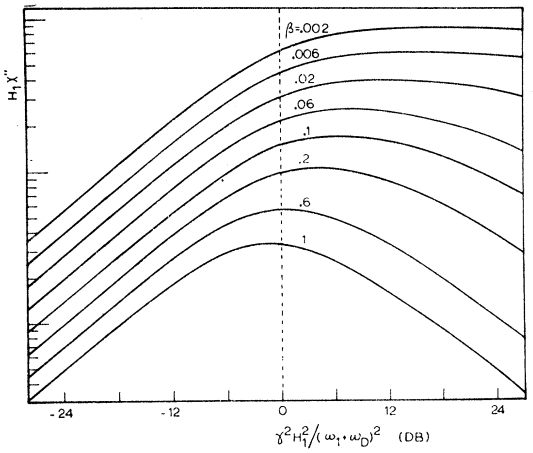

FIG. 1. Theoretical saturation curves [expression (2.13)] for values of β in the transition range.

We now assume $\omega=\omega_0$ and consider the saturation behavior. Figure 1 shows a family of saturation curves for various values of β. Some salient features of the saturation on Eq. (2.13) are as follows:

(1) If the spectral diffusion rate ω_D approaches zero then β approaches zero, and the expression is that given by Portis.[8]

(2) If $\omega_1<\omega_D\ll(\omega_1\omega_2^*)^{1/2}$, $\beta\ll1$, and the saturation plot differs only slightly from that in the usual inhomogeneous case, but saturation ($x=1$) occurs at $\gamma H_1=\omega_1+\omega_D$ rather than at $\gamma H_1=\omega_1$. For $\omega_D\ll(\omega_1\omega_2^*)^{1/2}$, a spectral diffusion event exchanges a hot spin on resonance for a lattice temperature spin away from resonance; this has the same effect on the population difference near the center of the line as does a spin-lattice relaxation event. That the spins scattered into the center from the wings are not, for $\beta\ll1$, appreciably hotter than the lattice temperature follows from the physical interpretation of the parameter β, as the probability that a hot spin scattered away from ω_0 will return before a spin-lattice event occurs. For $\beta\ll1$, the hot spins do not return, and hence returning diffusion brings in spins essentially at the lattice temperature.

(3) In the case $\omega_D\cong(\omega_1\omega_2^*)^{1/2}$, $\beta\simeq1$ and the βx^2 term in the denominator of (2.13) is dominant for $x\geq1$. The argument given above shows that a hot spin will scatter to within $\omega_1+\omega_D$ of any frequency in the line before relaxation. Hence the transition to homogeneous saturation behavior is essentially complete. This is reflected by the saturation curve for $\beta=1$. In the limit $\omega_D\gg(\omega_1\omega_2^*)^{1/2}$ the parameter β is not useful, and $H_1\chi''$ becomes

$$H_1\chi''(\omega_0)=\frac{1}{2}\frac{\chi_0\omega_0}{\gamma\omega_2^*}\frac{\gamma H_1}{1+(\gamma H_1)^2/\omega_1\omega_2} \quad (2.14)$$

as one expects for a homogeneously broadened resonance of width ω_2^*.

For cases of spectral diffusion described by the above random model, the analysis shows that the rate $\omega_1+\omega_D$ can be measured, in the range

$$\omega_1 \leq \omega_D \leq (\omega_1\omega_2^*)^{1/2}, \tag{2.15}$$

i.e., a factor $(\omega_2^*/\omega_1)^{1/2}$ in diffusion rate, by saturation measurement. Experimental saturation curves of $H_1\chi''(\omega_0)$ can be compared with the family of Fig. 1 to determine the parameter β. The experimental value of H_1 corresponding to $x=\gamma H_1/(\omega_1+\omega_D)=1$ for that particular β then determines $\omega_1+\omega_D$. From the two independent experimental quantities β and $\omega_1+\omega_D$ one can get ω_1 and ω_D.

In cases where the measured quantity is the peak derivative signal $(d/dH)(H_1\chi'')$, an approximate expression for small βx is

$$\frac{d}{d\omega}[H_1\chi''(\omega)]_{\text{peak}} \propto \frac{x}{(1+x^2)^{1/2}+2\beta x^2+\frac{1}{2}\beta^2 x^4}. \tag{2.16}$$

In this expression, which includes the effect of small lineshape changes, β is evaluated at $\omega=\omega_p$ such that $(d/d\omega)h(\omega)$ is maximum. For a Gaussian $h(\omega)$

$$h(\omega)=\pi^{-1/2}\Delta^{-1}\exp[-(\omega-\omega_0)^2/\Delta^2], \qquad h(\omega_p)/h(\omega_0)=e^{-1/2}. \tag{2.17}$$

If the denominator term in x^4 can be neglected, then (2.16) has the form of expression (2.13) for $H_1\chi''$ with β replaced by 2β.

The simplified treatment presented thus far for saturation on the random spectral diffusion model shows how the two effects of principal interest come about: the role of spectral diffusion as an apparent spin-lattice relaxation process at low ω_D, and the transition to homogeneous saturation behavior at $\omega_D \simeq (\omega_1\omega_2^*)^{1/2}$. The approximations that have been made are that uncertainty broadening alone, neglecting any coherence effects, determines the spin-packet function $g(\omega)$; and that the envelope function $h(\omega)$ is broad compared with $g(\omega)$. The result of a density matrix calculation[22] in which these two approximations are not made, for the case of a Gaussian $h(\omega)$ is

$$H_1\chi''(\omega_0)=\frac{1}{2}\frac{\chi_0\omega_0}{\gamma}\frac{(\omega_1+\omega_D)}{\omega_2^*} \times \frac{xE(x)}{(1+x^2)^{1/2}+[\beta x^2-\omega_D/\omega_2^*]E(x)}, \tag{2.18}$$

$$E(x)=(1-\text{erf}\Omega)\exp\Omega^2,$$

$$\Omega^2=\pi(\omega_1+\omega_D)^2(\omega_2^*)^{-2}(1+x^2).$$

[22] Since this calculation serves mainly as a theoretical justification for assumptions made above, and does not give new insight into the effects on saturation for $\omega_D<\omega_2^*$ with which this paper is concerned, it is omitted. It is contained in the author's Ph.D. thesis, Ref. 37.

The function $E(x)$ comes from evaluating the integral[13] (2.9) and approaches unity for $(\omega_1+\omega_D)\ll\omega_2^*$. In the limit $\omega_D/\omega_2^*\gg 1$, one finds that the expression (2.18) for $H_1\chi''(\omega_0)$ reduces to that for a homogeneously broadened resonance whose width is proportional to $(\omega_2^*)^2/\omega_D$. This is the width one expects for a motionally narrowed resonance. In the case $(\omega_1+\omega_D)^2+(\gamma H_1)^2 \ll(\omega_2^*)^2$, expression (2.18) reduces to the earlier result (2.13) and is taken to justify its derivation.

B. Identification of Spectral Diffusion

We now discuss the degree of confidence one can have, in cases in which the transition in saturation is observed, that it arises from spectral diffusion. Suppose that saturation curves for $H_1\chi''(\omega_0)$ fit expression (2.13), and that by variation of an external parameter (such as the temperature) essentially the whole range $\beta\ll 1$ to $\beta\gg 1$ is observed. Further assume that variation of ω_1 in the region of transition from inhomogeneously broadened to homogeneously broadened saturation behavior is negligible.

The experimental curves are analyzed independently for β (the shape) and the value of γH_1, denoted $\gamma H_{1/2}$, corresponding to $x=1$. The model requires, however, that β and $\omega_1+\omega_D$ be related by definition (2.13). Hence, a log-log plot of β versus $\gamma H_{1/2}$ should be (if we are to identify $\gamma H_{1/2}=\omega_1+\omega_D$) asymptotic for $\omega_D>\omega_1$ to a line of slope two, and the intercept of this line at $\beta=1$ determines the coefficient $1/\omega_1\omega_2^*$. An independent measurement of $1/\omega_1\omega_2^*$ may come from saturation in the limit $\beta\gg 1$, using (2.14) or through independent knowledge of ω_1 and measurement of the inhomogeneous linewidth ω_2^*.

Two necessary conditions for an interpretation on the model, then, are the slope two and the correct intercept in a log-log plot of β versus $\gamma H_{1/2}$.

It should be pointed out that a transition arising from increasing level width ω_2 approaching ω_2^*[13] may be indistinguishable in the above test. In this case, however, the resonance line should begin to broaden as the saturation transition is completed. One should also note that $\beta\cong 1$ on this mechanism requires the value $\omega_2=\omega_2^*$, which is larger than the corresponding rate $\omega_D=(\omega_1\omega_2^*)^{1/2}$ in the diffusion model by the factor $(\omega_2^*/\omega_1)^{1/2}$.

A second ambiguity occurs when the inequality

$$\omega_1<\omega_D<\omega_2<\omega_2^* \tag{2.19}$$

is satisfied; i.e., the level width is determined by something other than lifetime broadening $\omega_1+\omega_D$. It is possible that this situation might satisfy the test outlined. The significance of the measured quantities would be

$$(\gamma H_{1/2})^2=\omega_D\omega_2, \qquad \beta=\omega_D\omega_2/\omega_1\omega_2^*. \tag{2.20}$$

Finally, we speculate that in a case of spectral diffusion where there exists a distribution of steplengths having an rms value $\Delta\omega_j$, as long as the inequalities $\Delta\omega_j \gg \omega_D$ and $(\omega_D/\omega_1)^{1/2}\Delta\omega_j \gg \omega_2^*$ are satisfied, the analysis given above will describe the data. A special case in which $\Delta\omega_j \ll \omega_D$ has been treated and gives saturation behavior[23] which would not be confused with that described above.

III. EXPERIMENTAL

This section contains a brief description of the ESR spectrometer, the high-temperature microwave cavity, and the procedures used in preparing samples and in reducing data.

A. Electron Spin Resonance Spectrometer

The spectrometer is of conventional design, operates at about 9.5 Gc sec, and employs balanced bolometer detection. A Varian V-58 klystron, which is stabilized to a separate reference cavity, at full power of 400 mW gives a rotating H_1 at the sample of 0.8 G, corresponding to $\gamma H_1 = 1.4 \times 10^7$ rad/sec. A Narda power meter is used to monitor the power incident on the sample cavity. The phase of the microwave bolometer bias is adjusted to make the system sensitive only to the absorption signal $H_1\chi''$. The balance of the microwave bridge is displayed on an oscilloscope during data taking, and fine adjustments of the klystron frequency, nulling out any dispersion mode, are made by hand. Sinusoidal modulation of the magnetic field H_0, usually of 4 G amplitude, is at 35 cps; the output of the 35 cps lock-in amplifier following the bolometer detectors is thus proportional to $(d/dH)(H_1\chi'')$. The gain of the spectrometer detection system was observed to vary by less than 5% during the half hour required for a typical set of saturation measurements.

B. High-Temperature Cavity

One of the prime considerations in designing the cavity system was isolation of the KCl sample from any source of contamination. This is of particular importance at high temperatures where diffusion becomes rapid. The cavity shown in Fig. 2 minimizes contamination by placing the sample in a quartz tube, in contact only with hot flowing dry nitrogen. The cavity interior is sealed with O-rings as shown and evacuated to less than 10^{-5} Torr with a diffusion pump, so that the cavity walls always remain cool. Some advantages of this are that the resonant frequency, Q and coupling to the waveguide of the sample cavity change very little with temperature; and that the relatively small thermal mass of the sample and quartz tube allows temperature changes to be made quickly. The interior surfaces of the cavity are gold plated to improve the radiation shielding of the sample and to insure long-term constancy of the cavity characteristics.

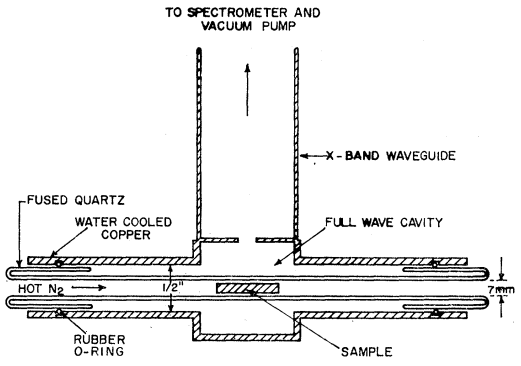

FIG. 2. High-temperature microwave cavity, showing the quartz Dewar tube, sample position, and flow of hot nitrogen gas.

[23] P. R. Moran, Phys. Rev. (to be published).

The sample temperature is determined by a Chromel-P-Alumel thermocouple spaced a fixed distance of about a centimeter behind the crystal on a quartz probe assembly. A separate calibration was carried out to find the sample temperatures corresponding to readings of the probe assembly thermocouple. The dry-nitrogen flow rate is maintained at 15 liters/min. A temperature controller holds the mean sample temperature constant to within 2°C at 500°C during the time required for a saturation run. The uncertainty in measurement of the sample temperature is estimated as ±10°C at 500°C, and less than ±5°C below 500°C, limited by an increasing temperature gradient along the sample above 500°C. An annoying feature of this system at high power is a tendency toward a $g=2$ cyclotron resonance discharge in the evacuated region of the cavity at the highest temperatures. For high-temperature $g=2$ operation above 1 W a scheme of surface treatment or of baffles to reduce the mean free path would possibly cure this tendency.

C. Data Reduction

All data were corrected in a uniform way for variations in klystron power, for small variations in the mean amplitude H_1 over crystals of varying lengths, and for loss of signal during a run because of thermal bleaching. A by-product of this procedure was an estimate of the diffusion constant for the F centers, at the highest temperatures used.

The raw data on a particular sample consisted, first, of a history of temperature versus time for the periods during which the crystal was heated above room temperature. The data for a saturation run at a particular temperature consist of derivative line shapes on the recorder paper for different values of incident power H_1^2 spaced at 3 or 6 dB intervals. In order to check for variations in spectrometer gain or for loss of signal by thermal bleaching, the line was displayed twice at each power with a 10- or 15-min interval between corresponding displays.

At temperatures above 500°C thermal bleaching led to a decrease in the observed signal, for fixed power,

typically of more than 5% over the half-hour duration of a particular saturation run. This decay limits the upper temperature at which saturation measurements can be made, for a given sample size.

Analysis of a saturation run consisted of fitting the signal decay at constant power to an exponential law $S=S_0\exp(-\alpha t)$, and then correcting all signal levels back to the time at which the run started. The corrected peak-to-peak derivative signals were measured and plotted on semi-log paper versus H_1^2 in decibels. Relaxation rates were assigned to high temperature saturation plots by comparison with the family of curves in Fig. 1.

The error introduced by analyzing data on expression (2.13) rather than expression (2.16) appropriate for the peak derivative is not judged to be important for $\beta\leq 0.5$ and the x values experimentally attained. The meaning of an experimentally determined β is correspondingly

$$\beta=2(\omega_D(\omega_1+\omega_D)/\omega_1\omega_2^*)e^{-1/2}. \tag{3.1}$$

Saturation curves taken at room temperature did not fit this family, and $H_{1/2}^2$ was assigned using the empirical shape for quenched samples at room temperature given by Moran, Christensen, and Silsbee.[9] A relative calibration of H_1^2 was accomplished by comparing $H_{1/2}^2$ for freshly quenched samples at room temperature with the measurements of Portis[8] and Seidel.[5] It was normally possible to estimate $H_{1/2}^2$ to ± 1 db, corresponding to about 15%, for F concentrations exceeding 3×10^{17}/cc.

D. Samples

The electron spin resonance samples were square in cross section 5 mm×5 mm and between 1 and 1.5 cm long. These were cleaved from Harshaw optical-quality KCl blocks or shaped from pieces of zone-refined KCl obtained from Professor Robert Pohl. The zone-refined pieces were polycrystalline, with single crystal regions typically a few millimeters in dimension. The zone-refined KCl contains divalent ion concentrations, as measured by ionic conductivity, better than a factor of 10 smaller than in Harshaw material, and shows no optical absorption at 204 mμ. ESR examination at 4.2°K of a zone-refined sample, after coloration and subsequent high-temperature measurements, showed no trace of the O_2^- resonance. A few crystals were grown from melt to which between 10 and 1000 ppm of $CaCl_2$ had been added.

E. Coloring Procedure

The usual additive coloration procedure was to heat the KCl sample in a sealed Pyrex bomb into which a gram or so of Baker and Adamson potassium metal had been distilled in vacuum. The bomb was placed in a special furnace with two heater windings so that the temperature of the crystals and of the potassium metal could be independently controlled. The equilibrium density of F centers in the sample is nearly proportional to the vapor pressure of the potassium,[24] which is related to the temperature of the potassium in the bomb by the vapor-pressure measurements of Honig.[25]

At a crystal temperature of 600°, the time for a crystal of dimension 0.5 cm to become uniformly colored was about 10 h. When the bomb was removed from the furnace, it was cooled in a few minutes by placing it in a jet of compressed air. The Pyrex bomb was then broken open under weak red light and the crystals were transferred to a light-tight box in a desiccator. The coloring method of van Doorn[26] was employed in a few instances.

F. Quenching and Optical Measurements

The density of F centers was determined at room temperature from the optical absorption constant at the peak of the F band, by using the Smakula formula.[27] The absorption constant of a thin wafer of colored KCl, usually between 0.4 and 1.5 mm thick, cleaved (under red light) from the middle of one of the colored pieces was measured on a Cary Model 14 spectrophotometer. In one case of a particularly dark crystal it was not possible to measure the F density in this fashion since it was not possible to cleave a wafer sufficiently thin. A comparison of this sample with an identically sized sample of low enough concentration to be measured optically was made on the ESR spectrometer; the comparison indicated a density of 2×10^{18}/cc. Unless a sample was to be run in the ESR spectrometer immediately after coloration, it was quenched immediately before the run. (The colored samples doped with $CaCl_2$ were not quenched, however.) The quenching procedure was to heat the spectrometer-sized sample to 580°C for 3 min in air, and then quickly transfer it from the oven to a copper block at room temperature. Samples cooled in this way showed a ratio of M-center optical absorption to F center optical absorption between 0.01 and 0.1, depending upon the F-center concentration. After quenching, care was taken to keep light from the crystal, to avoid any photochemical conversion effects.[27]

IV. EXPERIMENTAL RESULTS

High-temperature relaxation measurements were made on a variety of pure KCl samples additively colored to densities between 3×10^{17} and 2×10^{18}/cc, and on a few colored samples containing added $CaCl_2$. The results for the saturation power $(\gamma H_{1/2})^2$ for pure samples show a "low-temperature process" giving $(\gamma H_{1/2})^2\propto T^2$ up to 250°C; and a rapidly increasing $\gamma H_{1/2}$ depending exponentially on $1/T$ above about 350°C. In the doped samples the exponential dependence on $1/T$ appears earlier, at temperatures as low as

[24] H. Rogener, Ann. Physik **29**, 386 (1937).
[25] R. E. Honig, RCA Rev. **18**, 195 (1957).
[26] C. Z. van Doorn, Rev. Sci. Instr. **32**, 755 (1961).
[27] C. Z. van Doorn, Philips Res. Repts. Suppl. 4 (1962).

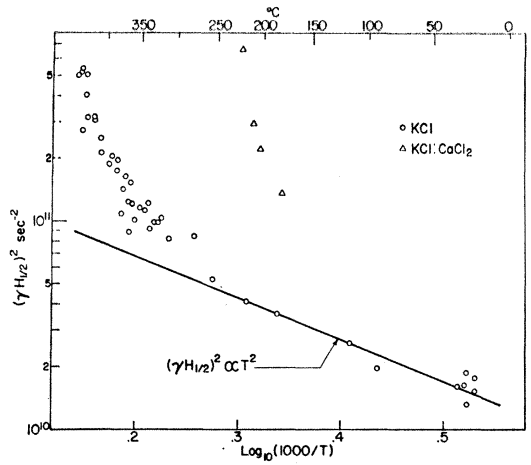

FIG. 3. Low-temperature relaxation data for pure samples (circles) and a $CaCl_2$-doped sample (triangles).

200°C. Systematic changes in saturation curve shape toward that appropriate for homogeneous broadening were observed in a doped sample above 240°C and in all pure samples above 470°C. Figure 3 gives a summary of the relaxation rate data for temperatures between 20° and 400°C, emphasizing the low-temperature process and showing the onset of the exponential process in several pure samples (circles) and one doped sample (the triangles). The value of $\gamma H_{1/2}$ was determined by comparison with the $\beta=0.02$ curve in Fig. 1, which was a good fit for all the data shown except for the points taken near room temperature, for which the saturation shape of Moran, Christensen, and Silsbee[9] was appropriate. It was necessary to quench the samples in order to obtain reproducible results below 100°C. The solid line drawn through the pure KCl data (the circles), which corresponds to $(\gamma H_{1/2})^2 \propto T^2$, fits within experimental error up to 250°C. The interpretation of the data, then, is consistent with a spin-lattice relaxation

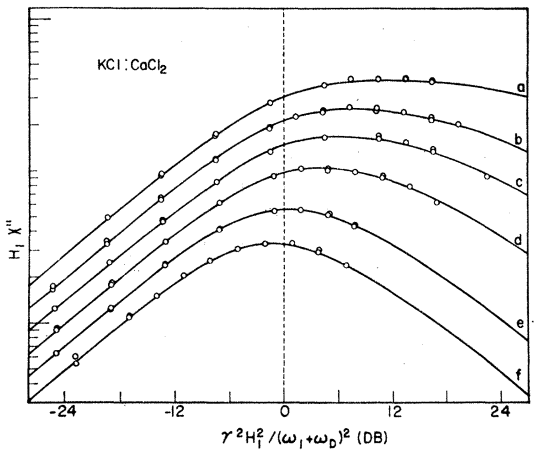

FIG. 4. Saturation curves from the $CaCl_2$-doped sample. Curves a to f correspond to β values of 0.02, 0.06, 0.1, 0.2, 0.6, and 1, and to ω_D values from 10^6 to 5.5×10^6 sec^{-1}.

rate ω_1 proportional to the square of the absolute temperature and a level width ω_2 independent of temperature. We can give further support to this interpretation after analysis of the data showing a transition to homogeneous saturation.

Figure 4 shows experimental saturation data (circled points) obtained on the $CaCl_2$-doped sample between 240 and 320°C, plotted in comparison with theoretical curves drawn from expression (2.13). The data plots clearly show a change in shape, well fit on the model of Sec. II for values of the shape parameter β between 0.02 and 1. The two-parameter data analysis outlined in II was therefore applied. The check of internal consistency justifying a two-parameter analysis is shown in Fig. 5. The straight line here is not simply the best line of slope2 but is drawn from expression (3.1) using the known value 3.4×10^8 sec^{-1} of ω_2*, the inhomogeneous linewidth, and an ω_1 obtained by extrapolation of the measurements of Feldman, Warren, and Castle[7] to the measurement temperature. The limiting form of the expression for ω_1 given by these authors for $T\gg210$°K is

$$\omega_1=3.5\times10^5(10^3/T)^{-2}\ \text{sec}^{-1}. \qquad (4.1)$$

Although the scatter in this plot is larger than can be accounted for from uncertainty in estimating β from the saturation plots,[28] the agreement obtained for $\beta\geq0.1$ without free parameters is taken as support for an interpretation in terms of spectral diffusion. The corresponding $\gamma H_{1/2}$ data are shown in Fig. 6, plotted in such a way that the exponential dependence $\gamma H_{1/2} \propto \exp(-U/kT)$ gives a straight line. This data, again disregarding

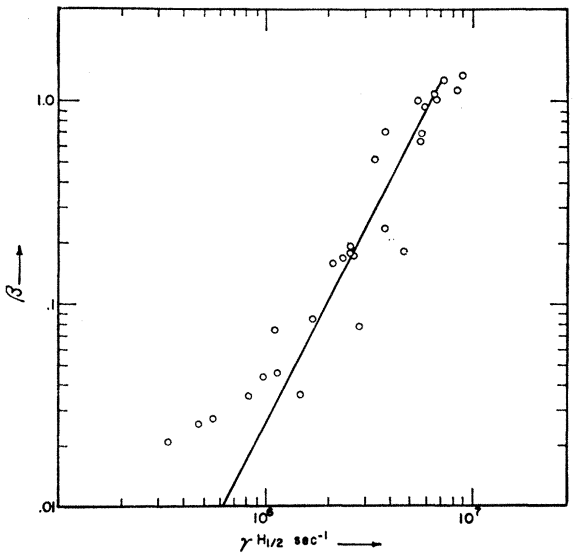

FIG. 5. Test of self-consistency of spectral diffusion analysis of data from the $CaCl_2$-doped sample. The solid curve corresponds to ω_1 from expression (4.1) and is regarded as a zero-parameter fit.

[28] This scatter appears related to variations in the ESR signal strength (measured at low H_1) suggesting partial equilibrium of dispersed F centers with a condensed colloidal phase showing no resonance.

scatter,[29] are what one would expect in going through the transition to homogeneous saturation as the result of an exponential spectral diffusion rate. The steeply rising $\gamma H_{1/2}$ on the low-temperature side is interpreted as $\gamma H_{1/2}=\omega_1+\omega_D$; the transition is complete at $10^3/T=1.7$, and the slow temperature variation on the high-temperature side of the transition (i.e., $\beta\gg1$) is determined by ω_1 alone, on expression (2.14). The dashed curve at the upper left is then

$$\gamma H_{1/2}=(2/\sqrt{e})^{1/2}(\omega_1\omega_2^*)^{1/2}$$

again drawn taking ω_1 values from the expression (4.1). [The constant $(2/\sqrt{e})^{1/2}$ represents the modification of (2.14) required for saturation of the peak derivative signal.] The width of the observed resonance in the region $\beta\gg1$ does *not* increase as would be expected on the alternative explanation of the transition, $\omega_2>\omega_2^*$. Further, in the latter case one would expect $\gamma H_{1/2}$ to continue to increase beyond $(\omega_1\omega_2^*)^{1/2}$, rather than the observed behavior. We conclude that an interpretation on the spectral diffusion model is correct, and regard the data at the upper left of Fig. 6 as a measurement of the spin-lattice relaxation rate confirming the expression (4.1) of Feldman *et al.*

The above conclusion does not depend on the details of the random spectral diffusion mechanism, e.g., the dependence of ω_D on temperature or on $CaCl_2$ content. The tendency of this system to form a colloid as studied by Heiland and Kelting[30] complicates quantitative measurements. There is a similarity, however, between the $\gamma H_{1/2}$ data and dc conductivity measurements on this system at high temperature.

In the case of pure KCl above 470°C, a similar transition occurs and does yield quantitative results. Saturation data plots obtained on several pure samples above 470°C are shown in Fig. 7. Data points are plotted along the best curves from Fig. 1, drawn from expression (2.13). The fit obtained on the spectral diffusion model is much better than the best possible on the Portis theory (the dashed curves).

In spite of the limited number of experimental points corresponding to $x>1$, it is possible in most cases to estimate β values. The log-log plot of β versus $\gamma H_{1/2}$ obtained by two parameter analysis of data from several samples is shown in Fig. 8. The line drawn in this plot is again not simply the best fit but is determined by the random diffusion model, expression (3.1), the room-temperature linewidth ω_2^*, and the expression (4.1). The general agreement (obtained *without* variation of any free parameters) is taken as strong support for interpretation on the random spectral diffusion model, and these data are correspondingly regarded as a measurement of ω_1 which within 20% agrees with the expression of Feldman *et al.*

Finally, a plot of the spectral diffusion rate ω_D obtained by the two-parameter analysis of data on several pure KCl samples is shown in Fig. 9. The data fit within estimates of systematic and random error to a straight line.

The data shown are essentially $\gamma H_{1/2}=\omega_1+\omega_D$ with ω_1 subtracted out. The range of ω_D has been extended in the lower decade by subtracting also contributions from the low temperature level broadening ω_2^e.[31] The

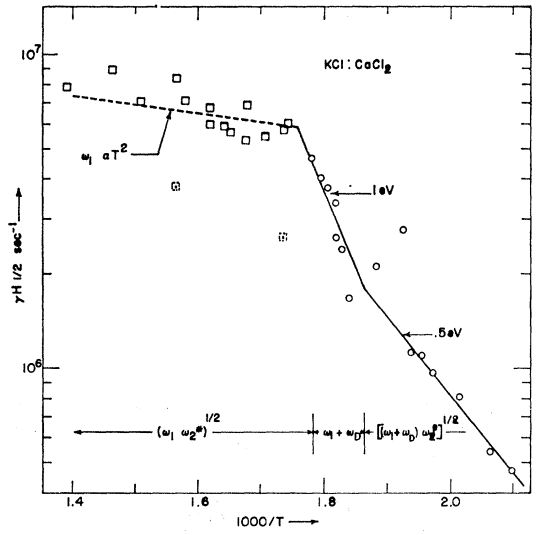

FIG. 6. $\gamma H_{1/2}$ data from two-parameter analysis of the $CaCl_2$-doped sample. The dashed curve at the upper left is drawn assuming homogeneous behavior, and is thus determined only by ω_1 and ω_2^*.

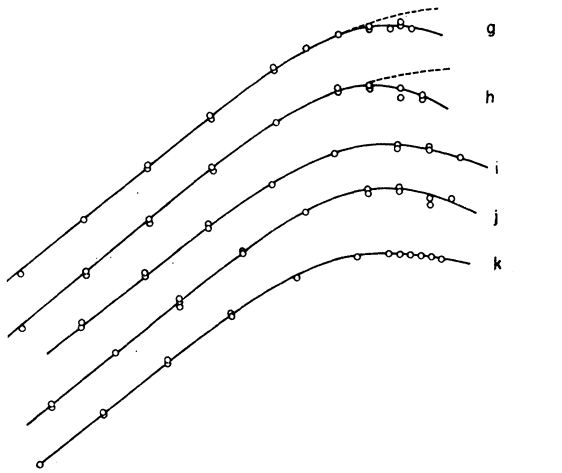

FIG. 7. High-temperature saturation plots on zone-refined pure KCl samples. These curves were taken in the temperature range 470 to 550°C on two samples: 8×10^{17}/cc (g, h, and j) and 2×10^{18}/cc (i and k). The dashed curves are the best fit possible on the Portis theory.

[29] A few points (the dashed squares) corresponding to large β have been corrected for variations in F-center signals, corresponding to varying amounts of colloid, on the assumption that ω_D is proportional to the dispersed F-center concentration.

[30] G. Heiland and H. Kelting, Z. Physik **126**, 689 (1949).

[31] The expression $(\gamma H_{1/2})^2=(\omega_1+\omega_D)(\omega_1+\omega_D+\omega_2^e)$ was solved for ω_D, taking ω_1 from (4.1) (about 2×10^5 sec^{-1}) and taking $\omega_2^e=5.5\times10^5$ sec^{-1} from the low-temperature saturation power divided by ω_1.

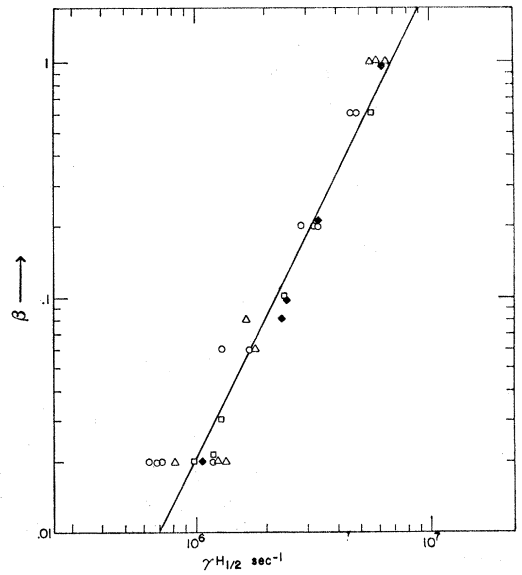

FIG. 8. Consistency test of spectral diffusion interpretation of data from several pure samples, Harshaw and zone refined. Zone-refined samples at 2×10^{18} and 8×10^{17} are represented by squares and triangles, respectively; a Harshaw sample at 5×10^{17} is represented by circles; and a crystal grown from Merck material is represented by diamonds.

correction varies from 2% at $\omega_D=10^7$ sec^{-1} to a factor two at $\omega_D=2\times10^5$ sec^{-1}.

Most of the data shown were obtained on a zone-refined KCl sample colored to 8×10^{17}/cc. Several points in the upper decade of ω_D were taken on Harshaw samples and cover a factor of 7 in F-density between 3×10^{17}/cc and 2×10^{18}/cc.[32]

Within experimental error the diffusion rate ω_D above 500°C is independent of F concentration and is the same for zone-refined and Harshaw KCl. These data, shown in Fig. 9, are therefore regarded as the result of an intrinsic process. The line best fitting the data corresponds to

$$\omega_D=\omega_D{}^0\exp(-U/kT)\,, \qquad (4.2)$$

where $U=1.6$ eV and $\omega_D{}^0=4.5\times10^{16}$ sec^{-1}. An estimate

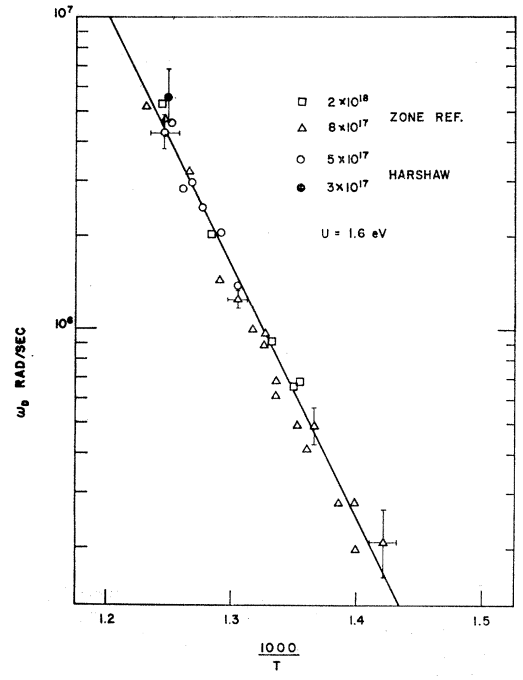

FIG. 9. High-temperature spectral diffusion rate from two zone-refined samples (triangles and squares), including highest temperature points from two Harshaw samples (see Fig. 10). This figure shows concentration *independence* of ω_D and equality of Harshaw and zone-refined sample above 500°C.

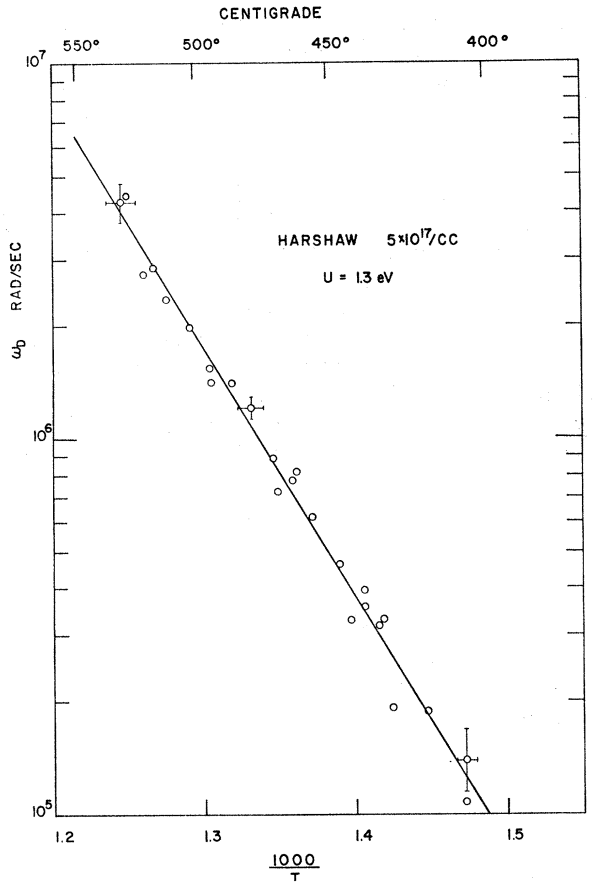

FIG. 10. Spectral diffusion rate for Harshaw sample 5×10^{17} including lower temperature points, which show ω_D exceeding that in zone-refined samples. The activation energy is 1.3 eV.

of the uncertainty in U is ±0.2 eV, which in turn makes $\omega_D{}^0$ uncertain by the large factor $10^{\pm1.2}$.

Below 500°C, Harshaw samples showed an enhanced spectral diffusion rate compared with the zone-refined sample. Data from a Harshaw sample colored to 5×10^{17}/cc are shown in Fig. 10. The activation energy

[32] Measurement of the ESR signal strength versus temperature showed that at 550°C very little colloid was present even in the 2×10^{18}/cc sample. Hence, the full factor seven in F-center density variation was realized.

here is 1.3 eV. Although the data here below 500°C show significantly larger ω_D than in the zone-refined sample, these points do *not* deviate when in the plot, Fig. 8, of β versus $\gamma H_{1/2}$. This fact is evidence that the deviations in ω_D are real, and is consistent with an added source of spectral diffusion in the Harshaw sample, probably related to the higher impurity levels.

It is of interest to compare the ω_D data with the diffusion constant of the F center as measured by the ESR signal loss rate. The signal decay rate is related to the F-center diffusion constant by treating the sample as a long cylinder of radius 2.5 mm and applying a solution of the diffusion equation with boundary condition N_F equals zero at the outer surface. The data are shown in Fig. 11. The activation energy for zone-refined samples is near 1.6 eV, while a lightly colored Harshaw sample has a smaller activation energy. The two zone-refined samples shown differ in initial F concentration by a factor 2.5 which is very nearly the factor by which the two data plots are shifted. There is thus a good indication that D_F varies *inversely* with F concentration above $N_F=8\times10^{17}$/cc and below 550°C. Under these conditions the F concentration exceeds the intrinsic vacancy concentrations.

We turn now to the question of mechanisms. From the good fit obtained using the random spectral diffusion model assuming the ω_1 of expression (4.1) put forth by Feldman *et al.*, we conclude that high-temperature relaxation in pure and doped samples results from spectral diffusion. It appears then that the spectral diffusion process contributes less than 20% of the value 2×10^5 sec^{-1} of ω_1, or less than $\frac{1}{2}$% of its value, to spin-lattice relaxation. We thus need search only for spectral diffusion mechanisms in what follows.

V. SPECTRAL DIFFUSION MECHANISMS

Three mechanisms producing spectral diffusion in the F center resonance, which should appear with rapid defect diffusion at high temperatures, are described. These are then discussed in relation to the pure KCl high-temperature data.

A. *F*-Center Step Diffusion

The F center diffuses one [110] step by exchanging positions with one of its 12 nearest-neighbor chlorine ions. After the jump the electron spin has changed four out of six nearest [100] potassium nuclei, seven out of 12 [110] chlorine neighbors, and all eight [111] potassium neighbors. One expects negligible correlation of nuclear M_I quantum members at neighboring sites. Hence, the resonant frequency of the F-electron spin is changed; the distribution of frequency-step lengths starting at ω_0 is nearly Gaussian with a width estimated as 0.7 to 0.8 ω_2*. The actual diffusion step is expected to be so sudden that spin-lattice relaxation is not an important result. In approximating the resulting spectral

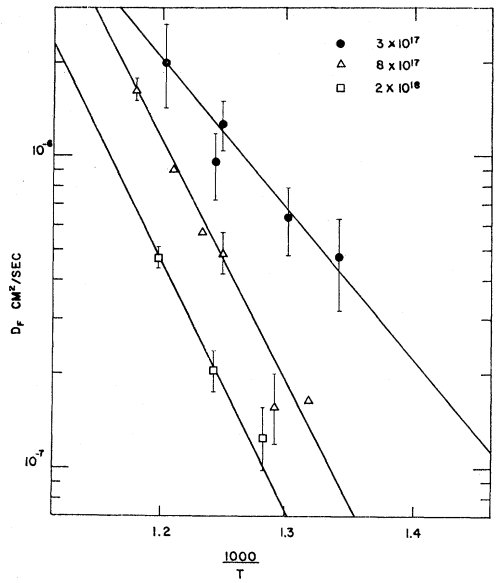

FIG. 11. Experimental estimate of D_F, the diffusion coefficient of the F center, based on the ESR signal loss rate. The two densely colored samples (zone-refined) show an activation energy near 1.6 eV, and give D_F values in the inverse ratio of the concentrations.

diffusion on the random spectral diffusion model, the diffusion rate is $\omega_D=12\nu_j$, where ν_j is the jump rate of the F center in a particular [110] direction. Hence, the temperature dependence of ω_D will be that of the thermally activated diffusion, $\nu_j=\nu_0\exp(-E_m/kT)$, where E_m is the energy for motion and ν_0 is a lattice frequency multiplied by an entropy factor. The spectral diffusion rate in this case is independent of the F center concentration as observed. Interpretation of the high-temperature zone-refined crystal ω_D data on this mechanism then requires $E_m=1.6\pm0.2$ eV and $\nu_0=3.7\times10^{15}\times10^{\pm1.2}$ sec^{-1}.

B. Conduction Electron Exchange

A process of thermal ionization of an F electron and its subsequent retrapping at an anion vacancy results in spectral diffusion which should be accurately described by the random model. A considerable enhancement of the associated spectral diffusion rate can occur in the case of dense coloration since the freed electron, in its diffusion toward an anion vacancy, typically encounters many other F centers. If the free electron exchanges positions (but not spin coordinates) with an electron bound at one of these F sites, a spectral diffusion event occurs.[33] An estimate of this enhanced spectral diffusion rate is the rate at which free electrons diffuse to within a critical exchange radius R_{cx} of an F center.

It is likely that the motion of the electron is character-

[33] D. Pines, J. Bardeen, and C. P. Slichter, Phys. Rev. **106**, 489 (1957). See also G. Feher and E. A. Gere, *ibid.* **114**, 1245 (1959).

ized by many scatterings in the time it takes to travel from one F center to another. Crude extrapolation of low-temperature electron mobility measurements[34] suggests that the mobility μ is of order of magnitude 1 cm^2/V sec in KCl at 500°C, corresponding to a mean free path not greater than a few times a, the nearest neighbor spacing. Hence the results obtained in the theory of diffusion limited reactions[35] appear appropriate in estimating the collision rates.

The corresponding expression for the exchange collision rate ω_x is

$$\omega_x = 4\pi D_e R_{cx} N_c, \tag{5.1}$$

where D_e is the diffusion coefficient for the conduction electron and N_c is the conduction-electron concentration. An estimate of the critical radius, R_{cx}, must be based on the cross section σ_x for the exchange process, which has been discussed in a similar context by Pines, Bardeen, and Slichter.[33] The matrix element for the exchange process involves the Coulomb interaction and is larger than that for various magnetic couplings. On a hydrogenic model, following Pines *et al.*, one finds

$$\sigma_x = (144\pi\hbar^4/m^2e^4)\epsilon^2, \tag{5.2}$$

where ϵ is the dielectric constant. Using the optical value $\epsilon = 2.1$ and an electronic mass, one finds $\sigma_x = 7\times10^{-14}$ cm^2 for KCl. The corresponding R_{cx} would be $R_{cx} = (\sigma_x/\pi)^{1/2}$ which is about $5a$, where a is the interionic spacing, 3.1 Å. For purposes of orientation we remark that the nearest neighbor spacing d_F at $N_F = 3\times10^{17}$/cc, given by $(4\pi/3)d_F{}^3 = (1/N_F)$,[36] is $30a$.

The effect of the exchange process on the saturation behavior can be verified in detail[37] by solving rate equations for the spins of both conduction and bound electrons, following the method of Pines *et al.* One finds that the expressions derived in Sec. II are valid, if one makes the identifications

$$\omega_1 \rightarrow \omega_1 + \omega_x \frac{\omega_c}{\omega_c + \omega_x N_F/N_c},$$
$$\omega_D \rightarrow \omega_x \frac{\omega_x N_F/N_c}{\omega_c + \omega_x N_F/N_c}. \tag{5.3}$$

Here ω_c is the spin-lattice relaxation rate for the conduction electron. The exchange process, then, contributes to both spectral diffusion and spin lattice relaxation. Since $\omega_x N_F/N_c$ is the rate at which a conduction electron experiences exchange collisions with F centers, the contribution to ω_1 of $\omega_x\omega_c(\omega_c+\omega_x N_F/N_c)^{-1}$ may be interpreted as the collision rate at an F center multiplied by the probability that the conduction electron will experience a spin-lattice collision before colliding with another F center. If $\omega_c \ll \omega_x N_F/N_c$, exchange collisions will lead predominantly to spectral diffusion. The conduction electron mechanism thus should result in a spectral diffusion rate proportional to the conduction electron concentration N_c. Comparison with the pure sample high-temperature data at 550°C requires, from (5.1), $N_c \cong 7\times10^{13}$/cc. Here D_e is estimated as 7×10^{-2} cm^2/sec using $\mu = 1$ cm^2/V sec and assuming the Einstein relation, and R_{cx} is taken as $5a$. The conduction electron concentration, on this interpretation of the ω_D data, would have to vary with an activation energy of 1.6 eV and be independent of the F-center concentration in the range 3×10^{17} to 2×10^{18} F center/cc. On the contrary, following the method of Mott and Gurney[38] (considering the thermal ionization of F centers, the formation of intrinsic vacancies and the requirement of charge neutrality), one finds

$$N_c \propto N_F \exp[-(U-\tfrac{1}{2}E_F)/kT], \tag{5.4}$$

where $U = 1.95$ eV[39] and $\frac{1}{2}E_F = 1.1$ eV. One expects then N_c proportional to the F concentration and showing an activation energy near 0.8 eV. Rough estimates assuming a normal parabolic conduction band give $N_c \sim 10^8$ electrons/cc at 550°C, for $N_F = 2\times10^{18}$/cc. One thus concludes from a simple theoretical estimate that the electronic mechanism cannot account for the observed data.

C. Vacancy Spectral Diffusion

Diffusion of a cation[40] vacancy through the vicinity of an F center rearranges the nearby ions so that afterward the electron spin interacts with a new set of nuclei, and hence the local field and resonant frequency are changed. The spectral diffusion resulting from such an event is characterized by a discrete set of frequency steps corresponding to the hyperfine constants with nuclei in the near-neighbor shell, which are listed in Table I. We expect that an encounter in which a cation vacancy visits four or five sites among the 14 [100] and [111] nearest-neighbor positions will produce a distribution of resonant frequencies sufficiently broad as to give the behavior outlined in II.

TABLE I. Hyperfine constants a for the KCl F center.

Direction	Shell	Nucleus		a(rad/sec)$\times10^{-6}$ [a]
[100]	I	K	(6)	129.4
[110]	II	Cl	(12)	43.3
[111]	III	K	(8)	2.0
[200]	IV	Cl	(6)	6.7
[210]	V	K	(24)	···
[211]	VI	Cl	(24)	0.6

[a] W. C. Holton and H. Blum, Phys. Rev. **125**, 89 (1962).

[34] A. G. Redfield, Phys. Rev. **98**, 1787 (1955).
[35] T. R. Waite, Phys. Rev. **107**, 463 (1957).
[36] S. Chandrasekhar, Rev. Mod. Phys. **15**, 1 (1943).
[37] E. L. Wolf, Ph.D. thesis, Cornell University, 1964 (unpublished). Cornell Materials Science Center Report #283.
[38] N. F. Mott and R. W. Gurney, *Electronic Processes in Ionic Crystals* (Clarendon Press, Oxford, England, 1948).
[39] This number was obtained by Mott and Gurney by analysis of the data on drift of F centers in an electric field, reviewed in Ref. 12.
[40] We neglect effects of the more slowly diffusing anion vacancies.

Since a short-range classical attractive force exists between the F center and a vacancy (of either sign) arising from the electronic polarizability α of the F center, it is considered reasonable to define a critical radius R_{cv} such that appearance of a vacancy at this radius insures a random spectral diffusion event. The estimate of ω_D, based on the diffusion limited reaction rate theory, is then

$$\omega_D = 4\pi D_v R_{cv} V^+, \tag{5.5}$$

where D_v and V^+ are, respectively, the diffusion coefficient and concentration of cation vacancies.[41]

We take R_{cv} as the radius at which the radial distribution $4\pi r^2 \exp[\epsilon_b(r)/kT]$ is maximum. In the field $E=e/\epsilon r^2$ of a vacancy at radius r the center develops a dipole moment p of magnitude αE, where α, the electronic polarizability, is estimated to be $\alpha = e^2\hbar^2/mU_0^2 = 1.7\times10^{-23}$ cm^3 if U_0 is the optical transition energy of 2.3 eV. The binding energy is then $\epsilon_b = \frac{1}{2}\alpha E^2 = \frac{1}{2}\alpha e^2/\epsilon^2 r^4 = \epsilon_0(a/r)^4$, where ϵ_0 is 0.5 eV assuming the optical dielectric constant $\epsilon = 2.1$. This gives $R_{cv} = 1.9a$; a generous estimate $R_{cv} = (\sqrt{5})a$ would include the [210] sites.

We estimate ω_D using D_v and V^+ as compiled from ionic conductivity measurements by Dreyfus and Nowick,[42] and using the relation[43] $D_v = 4\nu^+ a^2$, where ν^+ is the jump rate for the cation vacancy in a particular [110] direction. The values are

$$V^+ = (2a^3)^{-1} 35 e^{-E_f/2kT} \text{ cm}^{-3}, \tag{5.6}$$

and

$$\nu^+ = 1.2\times10^{14} e^{-E_m^+/kT} \text{ sec}^{-1}, \tag{5.7}$$

where

$$E_f = 2.2 \text{ eV} \quad \text{and} \quad E_m^+ = 0.8 \text{ eV}.$$

Thus one finds

$$\omega_{DV} = 2.3\times10^{17} \exp[-(E_m^+ + \tfrac{1}{2}E_f)/kT] \text{ sec}^{-1} \tag{5.8}$$

taking $R_{cv} = (\sqrt{5})a$. Evaluated at 550°C this gives $\omega_{DV} \cong 5\times10^5$ sec^{-1}, which is lower than the observed value by an order of magnitude. It is unlikely that R_{cv} should greatly exceed $(\sqrt{5})a$; hence we conclude that the vacancy mechanism does not account for the high-temperature zone-refined data.

D. Discussion of Mechanisms

Analysis of the high-temperature relaxation data has shown that the relaxation results from spectral diffusion in the F center resonance. Such spectral diffusion, implying a large change in the local hyperfine field of an F electron after a meantime $1/\omega_D$, can result only from motion of the electron from site to site, or by rearrangement of the nuclei near a particular site. It is therefore possible to choose the correct mechanism from these described by a process of elimination, if the estimates of the vacancy and conduction electron mechanisms are based on correct assumptions. On this basis the step diffusion mechanism must account for the observed data, since the conduction electron mechanism should give $\omega_D \propto N_F$, contrary to observation, and the vacancy mechanism, for which the numerical estimate should be accurate, is too slow.

Although the assignment of the spectral diffusion mechanism is unchanged, the ESR signal loss rate requires a numerical electron concentration N_c *not* in agreement with the theoretical estimate made above. In spite of uncertainty in the mechanism of electron production, however, it is still possible to rule out the electron exchange mechanism on the basis of the lack of observed N_F dependence. We turn to the macroscopic diffusion constant for the F center, D_F, as shown in Fig. 11. The values obtained, of the order of 10^{-6} cm^2/sec at 550°C, cannot result from the step diffusion process. For the jump rate ν_j of the F center cannot exceed $\omega_D/12$, and this would give $D_F = 4\omega_D a^2/12$, which is of order 10^{-9} cm^2/sec at 550°C.

The following simple model is proposed, which appears to explain the order of magnitude and dependence $D_F \propto 1/N_F$ in the limit of dense coloration.

Suppose that macroscopic diffusion is the result of a process of ionization of an F-center electron, which quickly diffuses a distance d_v to the nearest anion vacancy and is retrapped. This represents a charge flow; the charge imbalance must be compensated to avoid developing an electric field which would stop the further diffusion of electrons. We therefore assume that for each electron diffusing out, a cation vacancy diffuses back into the more densely colored region, and that this compensating step limits the diffusion rate. Thus the time required to move an F center by a distance d_v is $\tau_v = (1/12\nu^+)(d_v/a)^2$, where ν^+ is the jump rate of the cation vacancy, and $4\pi/3(d_v^3) = 1/V^+$. After N_F/V^+ such transfers, each taking time τ_v, each F center has advanced a distance d_v. The diffusion coefficient D_F is then of order $(V^+/N_F)12\nu^+a^2$. Using the intrinsic V^+ from (5.6), this expression does give the right order of magnitude for D_F, an activation energy of 1.9 eV compared with the very approximate 1.6 eV observed, and gives a natural understanding of the inverse dependence of D_F on the F-center concentration.

The assumption has been that the flow of electrons does not limit the diffusion. This permits a rough lower bound estimate of the electron concentration, N_c, if we use the Einstein relation and the order of magnitude estimate $\mu \approx 1$ cm^2/V sec for the electronic mobility. If charge compensation did not limit the diffusion, the

---

[41] This formula may be understood from a simple random walk argument. Let d_v be the distance to the nearest-neighbor vacancy, given by $(4\pi/3)d_v^3 = (V^+)^{-1}$ and note that $D_v = 4\nu^+a^2$. Then the diffusion limited rate is the inverse of the time $\tau_v = (1/12\nu^+)(d_v/a)^2$ to diffuse to a distance d_v, multiplied by the probability $\sim R_{cv}/d_v$ of actually intercepting a sphere of radius R_{cv} at radius d_v in an extended random walk.

[42] R. W. Dreyfus and A. S. Nowick, J. Appl. Phys. Suppl. **33**, 473 (1962).

[43] A. B. Lidiard, in *Handbuch der Physik*, edited by S. Flügge (Springer-Verlag, Berlin, 1957), Vol. 20, p. 246.

estimate of D_F would be simply the electron diffusion coefficient D_e multiplied by N_c/N_F, the fraction of the time the F center is ionized and free, in a sense, to diffuse. Hence,

$$D_F \leq D_e N_c/N_F \tag{5.9}$$

which implies $N_c/N_F \geq 3\times10^{-5}$ in order of magnitude at 550°C from Fig. 10. A similar estimate is possible from the drift rate of the F center in an applied electric field.[44] This would correspond to more than 10^{13} electrons/cc in the most heavily colored sample, as compared with the 10^8 electrons/cc estimated previously. While a complete understanding of the origin of the discrepancy is lacking, it is tempting to associate the extra electrons with the vacancy spectral diffusion mechanism. It is not unreasonable, in encounters in which a cation vacancy comes to the nearest [100] neighbor position of an F center, that the electron may be ionized.[45] An approximate rate equation for the conduction electron concentration might then be

$$dN_c/dt = 4\pi D_v R_{cv} V^+ N_F p - 4\pi D_e R_{ce} V^- N_c, \tag{5.10}$$

where p is a probability of ionization, R_{ce} is a capture radius for an electron of an anion vacancy, and V^- is the anion vacancy concentration. It is assumed that the vacancy pairs generated dissociate rapidly. If p has value unity, R_{cv} and R_{ce} have value $2a$, vacancy concentrations are intrinsic and D_e is 7×10^{-2} cm^2/sec, this equation implies a steady-state ratio N_c/N_F of about 10^{-4} at 550°C, in order of magnitude agreement with the experimental estimate. The electron concentration is proportional to N_F and has activation energy $E_m{}^+$ or 0.84 eV. From a thermal equilibrium viewpoint, the electron concentration is increased over that estimated previously because the energy to put an electron in the conduction band is now lowered by some fraction of the pair binding energy which has been calculated as 0.7 eV.[46] It is clear that this situation needs further study. On the other hand, we see no way in which the electron concentration at 550°C can be independent of the F center concentration. Hence the only acceptable interpretation of the data is on the step diffusion mechanism.

It is interesting to compare the values $E_m = 1.6$ eV and $\nu_0 = 3.7\times10^{15}\times10^{\pm1.2}$ sec^{-1}, implied for the F center diffusion process with corresponding values for similar defects. For the cation vacancy these are 0.84 eV and 1.2×10^{14} sec^{-1} [42]; for the anion vacancy 0.95 eV and 2.8×10^{14} sec^{-1}.[47] It is not surprising that the barrier energy for motion of the F center should exceed the values for the vacancies, since the electron is certainly less tightly bound in the saddlepoint configuration than in the F ground state, and this energy difference must be supplied in addition to the vacancy barrier energy to allow diffusion. It is not clear that ν_0 should exceed the values for the vacancies. However, the uncertainty ±0.2 eV in estimating the activation energy causes so large an uncertainty in ν_0 that a detailed consideration of this point is not justified.

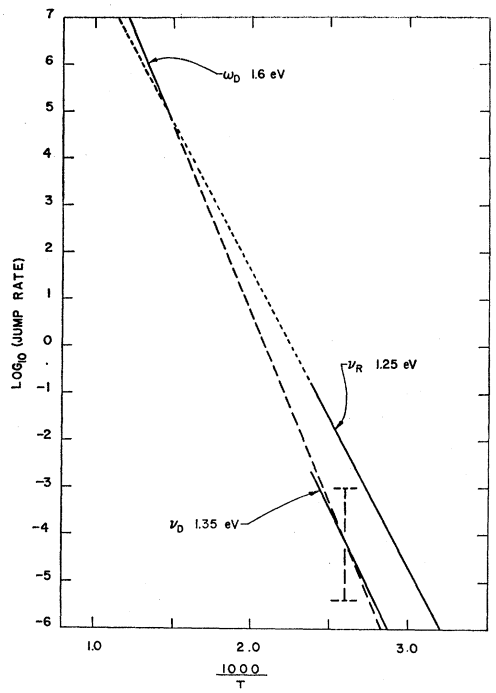

FIG. 12. Comparison of the spectral diffusion data with the F_A center disssociation (ν_D) and reorientation (ν_R) rates. The dashed error bar indicates the uncertainty in extrapolation of ω_D arising in the ±0.2 eV activation energy uncertainty.

A second comparison is possible with the reorientation and dissociation rates ν_R and ν_D of the sodium F_A center in KCl[48] measured by Lüty. An F_A center is an F center with a sodium ion as a [100] nearest neighbor. This defect has an optical absorption resolved from the F band, and it can be aligned optically leading to dichroism. The thermal rates for loss of dichroism and loss of F_A absorption have been interpreted, respectively, as the rates at which the F center jumps around and away from the sodium ion. As such these rates should have activation energies and attempt frequencies similar to ν_0 and E_m. A comparison of these rates is afforded in Fig. 12. It is seen that the slopes of ν_R and ν_D, 1.25 and 1.35 eV, respectively,[48] are lower than the 1.6 eV we obtain, and hence when extrapolated to 550°C ν_R and ν_D are lower than ω_D. On the other hand, extrapolation of ω_D to the temperatures around 100°C at which the optical measurements were made gives a value

[44] J. C. Gravitt, G. E. Gross, D. K. Benson, and A. B. Scott, J. Chem. Phys. **37**, 2783 (1962).

[45] A theoretical indication that a vacancy pair binds an electron only weakly is given by L. Pincherle, Proc. Phys. Soc. (London) **A64**, 648 (1951). Experimentally, such a complex, analogous to an F_A center, has not been observed optically, nor in the ENDOR study of the Z_1 center (roughly, the present complex associated with a divalent ion) of J. C. Bushnell, Ph.D. thesis, University of Illinois (unpublished).

[46] M. P. Tosi and F. G. Fumi, Nuovo Cimento **7**, 95 (1958).

[47] R. Fuller (private communication).

[48] These results were kindly communicated before publication by Dr. Fritz Lüty.

intermediate to ν_R and ν_D. It is thought that ν_R should exceed ω_D by virtue of a lower barrier energy, since the sodium ion is smaller than a potassium ion, presumably resulting in a general loosening of the lattice nearby. For this reason the increased value of ω_D at 550°C relative to the extrapolated ν_R is somewhat disturbing. It would seem however that no conclusion can be drawn because of the extreme sensitivity to small changes in the value of the activation energy for ν_R. On the whole, then, the comparison with ν_R and ν_D is considered to be satisfactory. The increased relaxation in the Harshaw sample, giving 1.3 eV, is assumed to result from higher impurity concentrations and is attributed to either the vacancy or the exchange mechanism. At the lower temperatures, the F concentration is fixed by equilibrium with colloid, and thus no test of concentration dependence is possible.

VI. CONCLUSIONS

It appears possible to draw the following conclusions from the work presented in the paper:

First, we have shown that spectral diffusion in an inhomogeneously broadened resonance of a suitably random nature, typified by a spin diffusing among sites having unrelated local fields, can lead to a well-characterized transition from inhomogeneously broadened to homogeneously broadened saturation behavior. In the transition range, $\omega_1 \leq \omega_D \leq (\omega_1\omega_2{}^*)^{1/2}$, the saturation data can be analyzed for the values of the spin-lattice relaxation rate ω_1 and the spectral diffusion rate ω_D.

Second, the inhomogeneously broadened magnetic resonance of the KCl F center shows such a transition to homogeneous saturation in the range 470° to 550°C. Analysis of the saturation data shows that the spin lattice relaxation rate ω_1 at 500°C agrees to 20% with the experimental expression of Feldman, Warren, and Castle, which for $T \gg 210$°K may be expressed as $\omega_1 = 3.5\times10^{-1}T^2$ sec^{-1}. In the range from room temperature to 250°C, below the transition range, the saturation parameter $(\gamma H_{1/2})^2 = \omega_1\omega_2{}^e$ is proportional to T^2. We conclude that the formula for ω_1 is valid from room temperature to 550°C and that $\omega_2{}^e$ is a constant equal to 5.5×10^5 sec^{-1} from room temperature to 250°C. In pure samples a thermally activated spectral diffusion process dominates the relaxation above 400°C. For zone-refined samples this rate is given by

$$\omega_D = 12\nu_0 \exp(-E_m/kT) \text{ sec}^{-1},$$

where $E_m = 1.6\pm0.2$ eV and $\nu_0 = 3.7\times10^{15}\times10^{\pm1.2}$ sec^{-1}. This rate is independent of the F-center concentration in the range studied and arises from diffusion of the F center in [110] directions by steps of length $\sqrt{2}a$, with an attempt frequency ν_0 and motion energy E_m. Greatly enhanced spectral diffusion rates in samples containing added $CaCl_2$ indicates at least one additional spectral diffusion process involving cation vacancies or conduction electrons. The diffusion constant of the F center in pure samples, measured by the decay rate of the ESR signal, is not accounted for by the above step diffusion process but occurs by electron transfer to anion vacancies. For F-center concentrations exceeding the intrinsic vacancy concentration the diffusion rate is limited by a charge compensating flow of vacancies.

ACKNOWLEDGMENTS

The author wishes to express his appreciation to Professor Robert Silsbee for suggesting this problem and for his continuing interest and support. Professor Robert Pohl is to be thanked for his cooperation in providing zone-refined KCl samples. The author wishes to thank Dr. Fritz Lüty for kindly supplying experimental data prior to their publication. It is a pleasure to acknowledge informative discussions with Professor W. B. Fowler, Professor Robert Maurer and Professor D. Y. Smith and with Dr. P. R. Moran and Dr. R. Fuller. The support of the Advanced Research Projects Agency through the facilities of the Cornell Materials Science Center is gratefully acknowledged. The author is particularly grateful to Professor W. Dale Compton for his encouragement in the final stages of this work.